

## ARTICLE

## Micro-structure of PECVD Diamond Films by Slow Positron Beam

Yan Xu, Hui-min Weng\*, Bang-jiao Ye, Hai-yun Wang, Cheng-xiao Peng, Chuan-ying Xi, Bin Cheng, Xian-yi Zhou, Rong-dian Han

Department of Modern Physics, University of Science and Technology of China, Hefei 230026, China

(Dated: Received on April 27, 2005; Accepted on July 8, 2005)

The microstructure of diamond films was studied by slow positron beam and Raman spectroscopy. For the Raman spectroscopy experiment on diamond films, a high fraction of the  $sp^3$  hybridized bond was detected in samples. Positron annihilation spectra analysis further illuminated that the concentration and types of defects were different in each sample.  $S$ - $E$  curves of all samples showed that diamond crystal structures had obvious variation in each sample. These results indicated that positron annihilation spectroscopy was an effective means to measure microstructure of diamond films.

**Key words:** Diamond film, Defect, Slow positron, Diffusion

## I. INTRODUCTION

CVD diamond, as a new functional material, is a promising material for numerous applications, because of its excellent properties. Because the crystal lattice constant and surface energy of diamond is different from normal substrates (e.g. Si, Ni), the CVD diamond film is generally a polycrystal. The quantity of defects in these films influence their electrical and thermal properties [1-3]. Therefore it is necessary to understand the micro-structure of the CVD diamond films.

The positron annihilation technique is now a powerful method for the study of defect in metals and semiconductors [4]. In the last few years, defects in CVD diamond bulk have been studied by Positron Annihilation Life Spectrum (PAL). However, this technique cannot reveal the micro-structure of near surface about films. The aim of this work is to study defects of near surface and whole crystal of PCVD diamond films using slow positron and Raman spectrum. The results show that there is some amorphous carbon in these diamond films and that the micro-structures of different samples have significant differences.

## II. EXPERIMENTAL SECTION

The samples were supplied by the plasma laboratory of University of Science and Technology of China [5]. The diamond films were deposited by the hot cathode direct current discharge plasma chemical vapor deposition method. Details of this technique were reported elsewhere [5].

A slow positron beam system, at the Department of Modern Physics of University of Science and Technol-

ogy of China, was used to measure positron annihilation Doppler broadening as a function of positron energy ( $E$ ) between 0.5 and 16 keV. The vacuum of target chamber is  $1.33 \times 10^{-5}$  Pa. In each spectrum  $10^5$  counts were accumulated. The Spectra were characterized by the  $S$  parameter.  $S$  is the ratio of  $\gamma$ -ray counts in the central part of the 511 keV annihilation peak to the total counts contained in the whole peak. Trapping of positrons by defects results in a larger  $S$  parameter because of the decreased annihilation probability of the trapped positrons, with high momentum core electrons.

## III. RESULTS AND DISCUSSION

To express damage depth profiles,  $S$  parameter is ordinarily plotted as a function of incident positron energy  $E$ . Figure 1 shows the  $S$ - $E$  curve for the diamond films.

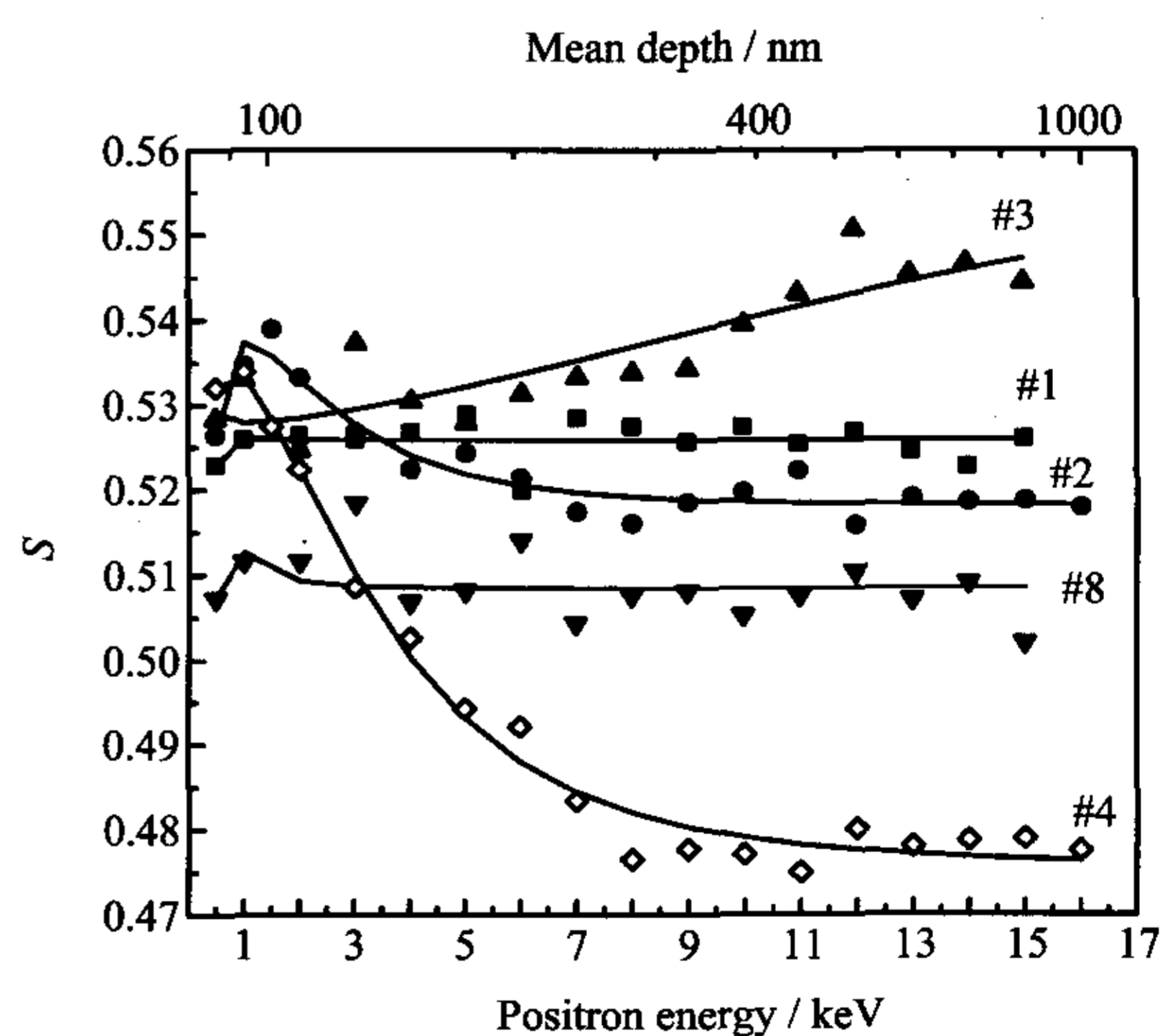


FIG. 1  $S$  parameter vs. positron energy  $E$  for the PECVD diamond films. — The best fitting.

A curve fit of the  $S$ - $E$  data was generated with

$$S = F_s S_s + F_b S_b + F_d S_d \quad (1)$$

\* Author to whom correspondence should be addressed. E-mail: wenghm@ustc.edu.cn

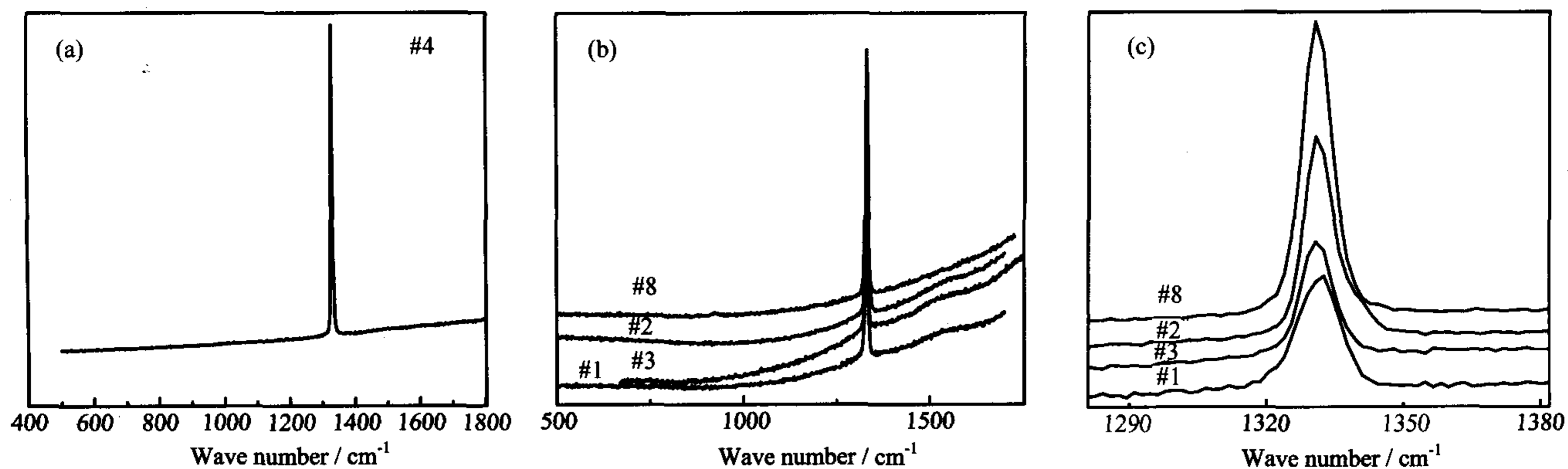


FIG. 2 The Raman spectra of the PECVD diamond films. (a). #4, (b). #1, #2, #3, #8, (c). The magnification of diamond peak.

and  $F_s + F_b + F_d = 1$ , where  $S_s$ ,  $S_b$  and  $S_d$  represent  $S$  values for surface, bulk, and defect, respectively.  $F$  represents the corresponding fraction of positrons being annihilated at the surface, trapped in the bulk and in defect.  $S_b$  and  $S_d$  were merged to  $S_t$ , because defects are uniformly distributed in our samples. So the measured  $S$  parameter is approximated by

$$S = F_s S_s + F_t S_t \quad (2)$$

$$F_s + F_t = 1 \quad (3)$$

Electronic momentum distributions vary in different phases and micro-structures. If there was lattice defect in the crystals, when a positron is annihilated predominantly by slow-moving electrons, the  $S$  parameter is larger. The use of the  $S$  parameter yields extensive information about defects and internal electric fields.

It is known that positrons diffuse over a fairly long distance after thermalization. The diffusion motion of the positron, in the absence of an electric field, is expressed by [6]

$$D_+ n''(z) - \frac{1}{\tau_{\text{eff}}} n(z) + P(z) = 0 \quad (4)$$

where  $D_+$  is the positron diffusion coefficient.  $n(z)$  is the positron density at the depth  $z$ .  $P(z)$  is the positron implantation profile.  $\tau_{\text{eff}}$  is the effective positron lifetime. The positron effective diffusion length,  $L_{\text{eff}}$ , is given by

$$L_{\text{eff}} = (D_+ \tau_{\text{eff}})^{1/2} = \left( \frac{D_+}{\lambda_b + \kappa_i} \right)^{1/2} \quad (5)$$

where  $\lambda_b$  is the positron annihilation rate from bulk material.  $\kappa_i = \mu_i C_i$ , where  $\mu_i$  is the proportionality coefficient.  $C_i$  is the defect concentration.  $S_s$ ,  $S_t$  and  $L_{\text{eff}}$  can be fitted using the VEPFIT program [7].

Table I contains the fitted results of all the samples. To determine the atomic bonding states of the carbon atoms, the samples were analyzed by Raman

TABLE I The fitting results of the samples

Sample number	$S_t$	$L_{\text{eff}}/\text{nm}$
#1	0.5259	3.01
#8	0.5085	4.03
#2	0.5180	51.45
#3	0.5385	28.58
#4	0.4755	85.69

spectroscopy. Figure 2 shows a series of Raman spectra of the diamond films.

As you can see, a sharp line dominates all the spectra. In addition, a flat background is found in the spectra (especially in the sample #4). The sharp peak at  $1332 \text{ cm}^{-1}$  is characteristic of  $\text{sp}^3$  bonding of the diamond form of carbon in the film [8]. The very broad peak center around  $1580 \text{ cm}^{-1}$  is attributed to the  $\text{sp}^2$  bonding of amorphous carbon. The Raman diamond peak of the #4 and the #8 samples, was more intense than that of other samples, which indicates that diamond crystalline of the #4 and #8 samples are better. In addition, we observe a broad peak center at around  $1580 \text{ cm}^{-1}$  in the Raman spectra of #1, #2, and #3 samples. This reveals that there are significant quantities of amorphous carbon in these three samples. The amorphous carbon peaks of the #1 and the #2 samples are flatter than that of the #3 sample. Whereas, the FWHM of the amorphous carbon peaks of the #1 and the #2 sample are larger than the #3 sample. This indicates there is less amorphous carbon in the #1 and the #2 sample. But we didn't find an amorphous carbon peak in the Raman spectra of #4 or #8 sample. The results of the Raman spectra for all the samples show that #4 and #8 samples have the highest fraction of  $\text{sp}^3$  bond, and that there is more amorphous carbon in the #3 sample compared to other samples.

To obtain more information on the micro-structure of the diamond films, we conducted the further measurements on the samples. Figure 1 and Table I repre-

sent the results of positron annihilation spectra and the curve fitting results.

The  $S$ - $E$  curve of the #4 sample is consistent with positron annihilation in a typical diamond crystal [9,10]. The measured  $S$  parameter of the #4 sample decreases quickly with positron energy until the bulk value is reached. This is a consequence of the fact that with increasing energy, and the positrons are implanted deeper inside the sample, meaning that fewer and fewer positrons will diffuse to and annihilate at surface. Almost all of the positrons implanted with energy higher than 8 keV annihilate in the film, giving a constant value of  $S$ . The effective diffusion length of 85.69 nm, for the #4 sample, is the largest of all the samples. According to Eq.(5), the defect concentration of the #4 sample is the lowest of all the samples.

The shape of the  $S$ - $E$  curve of the #2 sample is similar to that of the #4 sample, while its diamond phase content is far lower than that of the #4 sample. The fitted effective diffusion length  $L_{\text{eff}}$  of 51.45 nm for the #2 sample is smaller than that of the #4 sample (85.69 nm). This implies that the micro-structure of #2 sample is similar to that of the #4 sample.

Compared to the #2 and #4 sample, the  $S$ - $E$  curve of the #8 sample is very flat, which shows that the structure of #8 sample is not a typical diamond crystal structure, while it has a higher fraction of  $sp^3$  bond, only lower than that of #4 sample. Its effective diffusion length is only 4.03 nm, which is much smaller than that of #4 sample. The reason may be that compared to the #2 sample, and the #8 sample is a uniform film which is made up of smaller grains of diamond crystal. A positron is easily annihilated at the boundary of grain in the film. This results in a very small effective diffusion length for #8 sample. The structure of #1 sample is similar to #8 sample, the only difference being the diamond phase, which is lower than #8 sample due to the presence of amorphous carbon.

In the case of the #3 sample, significant amounts of amorphous carbon in the diamond film may lead to a differentiation of its  $S$ - $E$  curve from other samples. The free amorphous carbon exists in an amorphous state in the diamond crystal grain. Positron annihilation in that area is different from positron annihilation in diamond crystal region, which influences the value of  $S_t$ . The existence of amorphous carbon in a film will affect diffusion behavior of the positron. Sample #3 has an effective diffusion length  $L_{\text{eff}}$  of 25.58 nm.

The values of  $S_t$  for samples #1, #2 and #8, were 0.5259, 0.5180, 0.5085 respectively. Compared with the #4 sample, the increment  $\Delta S$  is 0.0494, 0.0425, and 0.033 for samples #1, #2 and #8 respectively. Thus the relative values are 10.4%, 9%, and 6.9%, respectively. This can be attributed to the fact that the defect size of the three samples is much larger than that of #4 sample. According to Eq.(5), smaller effective diffusion

length suggests a larger positron trapping rate, meaning a higher defect concentration. For the #1, #2, #4, and #8 samples, the defect concentration is the highest in the #1 and #8 samples, followed by the #2 sample, with the lowest in the #4 sample. Based on above analyses, we concluded that the crystal structure of the #4 sample is the best, as its defect concentration and defect size are the smallest. On the other hand, sample #3 has the poorest quality. Compared to the #8 sample, the defect concentration in #2 sample is much lower, and the crystal structure is better. The crystal structure of #1 and #8 are similar, only the diamond phase content is lower in the #1 sample.

#### IV. CONCLUSION

We have applied slow positron beam and Raman spectroscopy to investigate the microstructure of diamond films. We observed that the diamond films have a high fraction of  $sp^3$  hybridized bond and that there are different concentrations and sizes of defects in different samples. Positron annihilation spectroscopy is an effective means of measuring the microstructure of diamond films.

#### V. ACKNOWLEDGMENT

This work was supported by the National Natural Science Foundation of China (No.10425072) and the National High Technology Research and Development Program of China (2003AA84ts18).

- [1] S. Dannefear and W. Zhu, *Phys. Rev. B* **53**, 1979 (1996).
- [2] J. Rosa, J. Pangrác, M. Nesládek, *et al. Diamond Relat. Mater.* **7**, 1048 (1998).
- [3] M. Härting, M. Hempel and D. T. Britton, *Appl. Surf. Sci.* **149**, 170 (1999).
- [4] W. Z. Yu, *Positron Physics and Application*, Beijing: Science Press, (2003).
- [5] X. D. Zhu, H. Y. Zhou, R. J. Zhan, *et al. Appl. Surf. Sci.* **136**, 345 (1998).
- [6] H. M. Weng, X. Y. Zhou, B. J. Ye, *et al. Physics* **5**, 308 (2000).
- [7] A. Van Veen, *et al. AIP Conf. Proc.* **218**, 171 (1990).
- [8] E. H. Lee, D. R. Hembree, Jr. G. R. Rao and L. K. Mansur, *Phys. Rev. B* **48**, 15540 (1993).
- [9] I. Y. Al-Qaradawi, P. A. Sellin and P. G. Coleman, *Appl. Surf. Sci.* **194**, 29 (2002).
- [10] A. Uedono, S. Fujii and N. Morishita, *J. Phys. Condens. Matter.* **11**, 4109 (1999).